a low water solubility (precipitating near 10^{-4} M) and a critical micelle (or vesicle) concentration too small to measure. PNPDPP is hydrolyzed with a $k_{obsd} = 3.9 \times 10^{-3}$ s^{-1} (25.0 °C, pH 8.0) at exceedingly low A3 concentrations: 4.5×10^{-5} M. Binding of PNPDPP to A3 aggregates, estimated kinetically,[19] is also enzyme-like: $K_{assoc} = 4 \times 10^5$ M^{-1}. Although A3 has impressive rate and binding parameters, its low water solubility makes A3 less generally useful than its sibling.

Acknowledgment. This work was supported by the Army Research Office. We thank Dr. U. V. Venkataram for preparing the A2 ligand.

Stereoselective Formation of Rhodium and Iridium Hydrides via Intramolecular Hydrogen Bonding

Michael D. Fryzuk,*† Patricia A. MacNeil, and Steven J. Rettig‡

Contribution from the Department of Chemistry, University of British Columbia, Vancouver, British Columbia V6T 1Y6, Canada. *Received August 8, 1986*

Abstract: Dihydrogen addition to $Ir(CH_3)I[N(SiMe_2CH_2PR_2)_2]$ (R = Ph, *i*-Pr), under ambient conditions, results in protonation of the iridium amide bond to give an iridium amine monohydride complex, $IrH(CH_3)I[NH(SiMe_2CH_2PR_2)_2]$. $IrH(CH_3)I[NH(SiMe_2CH_2P(i\text{-}Pr)_2)_2]$ crystallizes in the triclinic space group $P\bar{1}$ with $a = 11.412$ (2) Å, $b = 14.712$ (3) Å, $c = 9.913$ (1) Å, $\alpha = 106.97$ (1)°, $\beta = 112.41$ (1)°, $\gamma = 70.99$ (1)° ($Z = 2$, $R_w = 0.040$). When these derivatives are heated under dihydrogen in toluene at 80 °C, the iridium amine dihydrides, $IrH_2I[NH(SiMe_2CH_2PR_2)_2]$, are produced. The analogous rhodium amides, $Rh(CH_3)I[N(SiMe_2CH_2PR_2)_2]$, yield only dihydride products, $RhH_2I[NH(SiMe_2CH_2PR_2)_2]$, under 1 atm of dihydrogen at room temperature. One of these, $RhH_2I[NH(SiMe_2CH_2P(i\text{-}Pr)_2)_2]$, has been crystallographically characterized; the complex belongs to the monoclinic space group $P2_1/n$ having the following cell dimensions: $a = 10.287$ (1) Å, $b = 21.317$ (1) Å, $c = 13.740$ (2) Å, $\beta = 110.296$ (6)° ($Z = 4$, $R_w = 0.034$). Reaction of $M(\eta^2\text{-}C_8H_{14})[N(SiMe_2CH_2PPh_2)_2]$ (M = Rh, Ir) with H_2 in the presence of CH_2X_2 (X = Cl, Br, I) also yields the amine dihydrides, $MH_2X[NH(SiMe_2CH_2PPh_2)_2]$. $IrH_2Cl[NH(SiMe_2CH_2PPh_2)_2]$, prepared by this route, was analyzed by X-ray crystallography and found to be a member of the monoclinic space group $P2_1/a$ with $a = 28.064$ (3) Å, $b = 10.817$ (1) Å, $c = 12.695$ (2) Å, $\beta = 97.27$ (1)° ($Z = 4$, $R_w = 0.039$). As shown by spectroscopic and crystallographic information, all of these M(III) amine hydride species possess a common structural feature: the amine N-H bond is syn to the metal-halide linkage. This orientation, as well as the concomitant stereoselectivity of these reactions, appears to be a direct consequence of intramolecular N-H···X hydrogen bonding.

An important structural feature in many organic compounds, especially those of biological significance, as well as a number of transition-metal complexes is the occurrence of hydrogen bonding;[1-5] such interactions are usually critically linked to stabilization and even reactivity of these species. With regard to hydrogen bonding in transition-metal derivatives, probably the most extensively studied[6-9] are the amine (amine ≡ ethylenediamine or ammonia) complexes of Co(III), Rh(III), Cr(III), and Ru(II), in which the outer-sphere interactions between the N-H moiety and the counterion (Cl^-, Br^-, I^-) are clearly demonstrated by both spectroscopic and X-ray diffraction data. More recently,[10] a series of crown-ether derivatives of W(0), Pt(II), Cu(II), and Co(III) amines have been prepared, in which the "soft" transition-metal center has been linked to the "hard" crown-ether via second sphere N-H···O hydrogen bonds; since crown-ethers do not readily bind to the later transition elements (due to mismatching of hard/soft[11] interactions), this is an indication of the stabilizing influence of hydrogen bonding. Other examples of such interactions in transition-metal systems are known[5] but are apparently fortuitous and have not been examined extensively.

A variety of spectroscopic techniques have been well utilized[3] for the assignment of such interactions. Traditionally, lowering of appropriate infra-red frequencies (ν_{NH} or ν_{OH}) or downfield shifts of ^1H NMR chemical shift values has been diagnostic. For transition-metal complexes containing π-acceptor ligands (such as CO or N_2), the decrease in $\nu_{\pi L}$ with increased outer-sphere hydrogen bonding can be a useful correlation.[8] Crystallographic analyses of a wide number of hydrogen-bonded transition-metal complexes[9] have shown significant shortening of the N-H···X distance (vs. sum of the van der Waals radii), the degree of contraction thus giving a useful approximation of the strength of these interactions. Solution spectroscopic information is usually insufficient to provide insight into the significance of these effects[12,13] since solvation sometimes results in breaking of these rather weak bonds.

In the course of our study of the coordination chemistry and reactivity of transition-metal amides, we discovered that a number of these rhodium and iridium species react with dihydrogen to

---

† Fellow of the Alfred P. Sloan Foundation (1984-1987).

‡ Experimental Officer: UBC Crystal Structure Service.

(1) Joesten, M. D.; Schaad, L. J. *Hydrogen Bonding*; Marcel Dekker: New York, 1974.

(2) Novak, A. *Struct. Bonding* **1974**, *18*, 177.

(3) Allen, L. C.; Kollman, P. A. *Chem. Rev.* **1972**, *72*, 283.

(4) Joesten, M. D. *J. Chem. Ed.* **1982**, *59*, 362.

(5) (a) Brunner, H.; Wachter, J.; Schmidbauer, J.; Sheldrick, G. M.; Jones, P. G. *Angew. Chem., Int. Ed. Engl.* **1986**, *4*, 371. (b) Newkome, G. R.; Frere, Y. A.; Fronczek, F. R.; Gupta, V. K. *Inorg. Chem.* **1985**, *24*, 1001. (c) Sakaguchi, U.; Tamaki, S.; Tomioka, K.; Yoneda, H. *Inorg. Chem.* **1985**, *24*, 1624 (d) Sutherland, B. R.; Cowie, M. *Organometallics* **1985**, *4*, 1637. (e) Bennet, M. A.; Rokicki, A. *Organometallics* **1985**, *4*, 180. (f) Fryzuk, M. D.; Jang, M.-L.; Jones, T.; Einstein, F. W. B. *Can. J. Chem.* **1986**, *64*, 174. (g) Cole-Hamilton, D. J.; Young, R. J.; Wilkinson, G. *J. Chem. Soc., Dalton Trans.* **1976**, 1995.

(6) Fujita, J.; Kobayashi, M.; Nakamoto, K. *J. Am. Chem. Soc.* **1956**, *78*, 3295.

(7) Osborn, J. A.; Powell, A. R.; Thomas, K.; Wilkinson, G. *J. Chem. Soc. A* **1968**, 1801.

(8) Chatt, J.; Leigh, G. J.; Thankarajan, N. *J. Chem. Soc. A* **1971**, 3168.

(9) Bronty, C.; Spinat, P.; Whuler, A. *Acta Crystallogr., Sect. B* **1980**, *36*, 1967.

(10) Colquhoun, H. M.; Lewis, D. F.; Stoddart, J. F.; Williams, D. J. *J. Chem. Soc., Dalton Trans.* **1983**, 607.

(11) Pearson, R. J. *J. Chem. Ed.* **1968**, *45*, 581, 643.

(12) Marcotrigiano, G.; Menabue, L.; Pellacani, G. C.; Saladini, M. *Inorg. Chim. Acta* **1979**, *32*, 149.

(13) Freeman, W. A. *Inorg. Chem.* **1976**, *15*, 2235.

0002-7863/87/1509-2803$01.50/0

Table I. ^{1}H NMR Data[a]

complex	$\mathrm{Si(C\mathit{H}_3)_2}$	$\mathrm{SiC\mathit{H}_2P}$	$\mathrm{N\mathit{H}}$	$\mathrm{P(C_6\mathit{H}_5)_2}$	other
$\mathrm{IrH(CH_3)I[NH(SiMe_2CH_2PPh_2)_2]}$	0.09 (s), −0.47 (s)	2.03 (dt, $J_{\mathrm{gem}} = 13.9$, $J_{\mathrm{ap}} = 4.8$), 2.63 (dt, $J_{\mathrm{app}} = 5.3$)	~2.6 (obscured by $\mathrm{C\mathit{H}_2P}$'s)	7.07 (m, para/meta), 7.72 (m, ortho), 8.07 (m, ortho)	Ir–H, −19.50 (t, $J_{\mathrm{P}} = 13.7$), Ir–CH_3, 1.31 (t, $J_{\mathrm{P}} = 6.7$)
$\mathrm{IrH(CH_3)I[NH(SiMe_2CH_2P(\mathit{i}\text{-}Pr)_2)_2]}$	0.11 (s), 0.29 (s)	obscured by $\mathrm{P\{CH(C\mathit{H}_3)_2\}_2}$	2.13 (s, br)		$\mathrm{P\{CH(C\mathit{H}_3)_2\}_2}$, 1.15 (m), 1.49 (m), $\mathrm{P\{CH(C\mathit{H}_3)_2\}_2}$, 2.18 (m), 3.39 (m), Ir–H, −21.41 (t, $J_{\mathrm{P}} = 14.5$), Ir–CH_3 (obscured by $\mathrm{P\{CH(C\mathit{H}_3)_2\}_2}$)
$\mathrm{IrH_2I[NH(SiMe_2CH_2PPh_2)_2]}$	0.13 (s), −0.36 (s)	2.26 (dt, $J_{\mathrm{gem}} = 13.3$, $J_{\mathrm{app}} = 4.4$), 2.44 (dt, $J_{\mathrm{app}} = 5.5$)	~2.4 (obscured by $\mathrm{C\mathit{H}_2P}$'s)	6.95, 7.07 (m, para/meta), 7.95, 8.08 (m, ortho)	Ir–H (trans to I), −19.39 (td, $J_{\mathrm{P}} = 13.2$, $J_{\mathrm{H}} = 7.9$), Ir–H (trans to NH), −23.10 (td, $J_{\mathrm{P}} = 15.0$)
$\mathrm{IrH_2I[NH(SiMe_2CH_2P(\mathit{i}\text{-}Pr)_2)_2]}$	0.02 (s), 0.17 (s)	1.22 (m)	2.36 (s, br)		$\mathrm{P\{CH(C\mathit{H}_3)_2\}_2}$, 1.04 (m), 1.12 (m), 1.49 (m), $\mathrm{P\{C\mathit{H}(CH_3)_2\}_2}$, 1.76 (m), 3.01 (m), Ir–H (trans to I), −21.97 (td, $J_{\mathrm{P}} = 15.2$, $J_{\mathrm{H}} = 7.8$), Ir–H (trans to NH), −25.25 (td, $J_{\mathrm{P}} = 14.2$)
$\mathrm{IrH_2Br[NH(SiMe_2CH_2PPh_2)_2]}$	0.14 (s), 0.29 (s)	2.29 (dt, $J_{\mathrm{gem}} = 13.8$, $J_{\mathrm{app}} = 7.0$), 2.40 (dt, $J_{\mathrm{app}} = 4.1$)	2.71 (s, br)	7.00 (m, para/meta), 8.03 (m, ortho)	Ir–H (trans to Br), −22.00 (td, $J_{\mathrm{P}} = 15.3$, $J_{\mathrm{H}} = 8.5$), Ir–H (trans toNH), −23.19 (td, $J_{\mathrm{P}} = 14.4$)
$\mathrm{IrH_2Cl[NH(SiMe_2CH_2PPh_2)_2]}$	0.25 (s), −0.14 (s)	2.22 (dt, $J_{\mathrm{gem}} = 14.6$, $J_{\mathrm{app}} = 4.5$), 2.32 (dt, $J_{\mathrm{app}} = 5.1$)	3.05 (s, br)	7.02 (m, para/meta), 8.00 (m, ortho)	Ir–H (trans to Cl), −23.06 (td, $J_{\mathrm{P}} = 14.3$, $J_{\mathrm{H}} = 7.9$), Ir–H (trans to NH), −23.24 (td, $J_{\mathrm{P}} = 14.5$)
$\mathrm{RhH_2I[NH(SiMe_2CH_2PPh_2)_2]}$	0.20 (s), −0.28 (s)	1.94 (dt, $J_{\mathrm{gem}} = 15.1$, $J_{\mathrm{app}} = 4.2$), 2.66 (dt, $J_{\mathrm{app}} = 5.5$)	2.78 (s, br)	7.01 (m, para/meta), 7.92 (m, ortho), 8.04 (m, ortho)	Rh–H (trans to I), −14.17 (m, $J_{\mathrm{Rh}} = 26.6$, $J_{\mathrm{P}} = 12.2$, $J_{\mathrm{H}} = 9.0$), Rh–H (trans to NH), −17.71 (m, $J_{\mathrm{Rh}} = 24.4$, $J_{\mathrm{P}} = 13.6$)
$\mathrm{RhH_2I[NH(SiMe_2CH_2P(\mathit{i}\text{-}Pr)_2)_2]}$	0.12 (s), 0.30 (s)	obscured by $\mathrm{P\{CH(C\mathit{H}_3)_2\}_2}$	2.55 (s, br)		$\mathrm{P\{CH(C\mathit{H}_3)_2\}_2}$, 1.10 (m), 1.20 (m), 1.55 (m), $\mathrm{P\{C\mathit{H}(CH_3)_2\}_2}$, 1.80 (m), 2.93 (m), Rh–H (trans to I), −16.64 (m, $J_{\mathrm{Rh}} = 29.6$, $J_{\mathrm{P}} = 14.2$, $J_{\mathrm{H}} = 9.1$), Rh–H (trans to NH), −19.75 (m, $J_{\mathrm{Rh}} = 24.9$, $J_{\mathrm{P}} = 14.0$)
$\mathrm{RhH_2Br[NH(SiMe_2CH_2PPh_2)_2]}$	0.15 (s), −0.28 (s)	1.82 (dt, $J_{\mathrm{gem}} = 14.68$ $J_{\mathrm{app}} = 4.1$), 2.47 (dt, $J_{\mathrm{app}} = 5.0$)	3.07 (s, br)	7.04 (m, para/meta), 8.00 (m, ortho)	Rh–H (trans to Br), −16.43 (m, $J_{\mathrm{Rh}} = 25.9$, $^2J_{\mathrm{P}} = 13.7$, $^2J_{\mathrm{H}} = 9.9$), Rh–H (trans to NH), −17.79 (m, $^1J_{\mathrm{Rh}} = (25.1$, $^2J_{\mathrm{P}} = 13.8$)
$\mathrm{RhH_2Cl[NH(SiMe_2CH_2PPh_2)_2]}$	0.16 (s), −0.23 (s)	1.81 (dt, $J_{\mathrm{gem}} = 13.9$, $J_{\mathrm{app}} = 4.8$), 2.39 (dt, $J_{\mathrm{app}} = 5.2$)	3.38 (s, br)	7.02 (m, para/meta), 7.94 (m, ortho), 8.06 (m, ortho)	Rh–H (trans to Cl), −17.59 (m, $^1J_{\mathrm{Rh}} = 24.5$, $^2J_{\mathrm{P}} = 14.5$, $^2J_{\mathrm{H}} = 10.3$), Rh–H (trans to NH), −17.80 (m, $^1J_{\mathrm{Rh}} = 25.6$, $^2J_{\mathrm{P}} = 13.0$)

[a] All ^{1}H NMR spectra were recorded at 400 MHz in C_6D_6 at room temperature. Chemical shifts (in ppm) are referenced to residual solvent protons (C_6D_5H at 7.15 ppm), and coupling constants (J) are in hertz.

Table II. Infrared N–H and N–D Stretching Frequencies[a]

complex	$\nu_{\mathrm{N-H}}$	$\nu_{\mathrm{N-D}}$	$\nu_{\mathrm{N-H}}/\nu_{\mathrm{N-D}}$	complex	$\nu_{\mathrm{N-H}}$	$\nu_{\mathrm{N-D}}$	$\nu_{\mathrm{N-H}}/\nu_{\mathrm{N-D}}$
$\mathrm{IrH_3[NH(SiMe_2CH_2PPh_2)_2]}$	3258 (m)	2418	1.347	$\mathrm{IrH(CH_3)I[NH(SiMe_2CH_2P(\mathit{i}\text{-}Pr)_2)_2]}$	3200 (m, br)	2405	1.331
$\mathrm{IrH_2Cl[NH(SiMe_2CH_2PPh_2)_2]}$	3140 (m, br)	2360	1.331	$\mathrm{RhH_2I[NH(SiMe_2CH_2P(\mathit{i}\text{-}Pr)_2)_2]}$	3170 (m, br)	2365	1.340
$\mathrm{IrH_2Br[NH(SiMe_2CH_2PPh_2)_2]}$	3140 (m, br)	2360	1.331	$\mathrm{RhH_2I[NH(SiMe_2CH_2PPh_2)_2]}$	3170 (m, br)	2370	1.338
$\mathrm{IrH_2I[NH(SiMe_2CH_2PPh_2)_2]}$	3170 (m, br)	2382	1.331	$\mathrm{RhH_2Br[NH(SiMe_2CH_2PPh_2)_2]}$	3160 (m, br)	2362	1.338
$\mathrm{IrH(CH_3)I[NH(SiMe_2CH_2PPh_2)_2]}$	3155 (m, br)	2365	1.334	$\mathrm{RhH_2Cl[NH(SiMe_2CH_2PPh_2)_2]}$	3142 (m, br)	2370	1.326

[a] Infrared spectra were recorded in CH_2Cl_2; stretching frequencies are in cm^{-1} (m ≡ moderate, s ≡ strong, br ≡ broad).

Table III. Crystallographic Data[a]

compd	$Ir(CH_3)I(H)[NH(SiMe_2CH_2P(i\text{-}Pr)_2)_2]$	$Rh(H)_2I[NH(SiMe_2CH_2P(i\text{-}Pr)_2)_2]$	$Ir(H)_2Cl[NH(SiMe_2CH_2PPh_2)_2]\cdot CH_3C_6H_5$
formula	$C_{19}H_{49}IIrNP_2Si_2$	$C_{18}H_{47}INP_2RhSi_2$	$C_{30}H_{39}ClIrNP_2Si_2\cdot C_7H_8$
fw	728.8	625.5	851.6
cryst system	triclinic	monoclinic	monoclinic
space group	$P\bar{1}$[b]	$P2_1/n$[c]	$P2_1/a$[c]
a (Å)	11.412 (2)	10.287 (1)	28.064 (3)
b (Å)	14.712 (3)	21.317 (1)	10.817 (1)
c (Å)	9.913 (1)	13.740 (2)	12.695 (2)
α	106.97 (1)	90	90
β	112.41 (1)	110.296 (6)	97.27 (1)
γ (deg)	70.99 (1)	90	90
V (Å^3)	1427.7 (4)	2825.9 (5)	3823.0 (7)
Z	2	4	4
D_{calcd} (g/cm^3)	1.696	1.470	1.479
$F(000)$	716	1272	1712
μ(Mo Kα) cm^{-1}	59.3	18.8	37.2
cryst dimensns (mm)	0.20 × 0.21 × 0.45	0.22 × 0.25 × 0.36	0.15 × 0.16 × 0.56
transmissn factors	0.271–0.422	0.642–0.695	0.522–0.625
scan type	$\omega-2\theta$	$\omega-2\theta$	$\omega-2\theta$
scan range (deg in ω)	$0.70 + 0.35 \tan \theta$	$0.65 + 0.35 \tan \theta$	$0.80 + 0.35 \tan \theta$
scan speed (deg min)	1.12–10.06	1.06–10.06	1.26–10.06
data collected	$\pm h, \pm k, -l$	$\pm h, +k, +l$	$\pm h, +k, +l$
maximum 2θ (deg)	60	55	55
cryst decay	4.5%	negligible	negligible
unique reflectns	8291	6463	8735
reflectns with $I \geq 3\sigma(I)$	5920	3979	4766
no. of variables	248	238	405
R	0.033	0.029	0.039
R_w	0.040	0.034	0.039
S	1.675	1.338	1.415
mean Δ/σ (final cycle)	0.03	0.02	0.03
max Δ/σ (final cycle)	0.27	0.23	0.37
residual density (e/Å^3)	−1.9 to +2.1	−1.6 to +0.8	−2.2 to +2.6

[a] Temperature 22 °C. Enraf-Nonius CAD4-F diffractometer, Mo Kα radiation (λ_{K1} = 0.70930, λ_2 = 0.71359 Å), graphite monochromator, takeoff angle, 2.7°, aperature ($2.0 + \tan \theta$) × 4.0 mm at a distance of 173 mm from the crystal, scan range extended by 25% on both sides for background measurement, $\sigma^2(I) = S + 2B + [0.040(S - B)]^2$ (S = scan count, B = normalized background count), function minimized $\sum w(|F_o| - |F_c|)^2$ where $w = 1/\sigma^2(F)$, $R = \sum||F_o| - |F_c||/\sum|F_o|$, $R_w = (\sum w(|F_o| - |F_c|)^2/\sum w|F_o|^2)^{1/2}$. $S = (\sum w(|F_o| - |F_c|)^2/(m - n))^{1/2}$. Values given for R, R_w, and S are based on those reflections with $I \geq 3\sigma(I)$. [b] Reduced cell, conventional orientation. [c] Alternate settings of $P2_1/c$ with equivalent positions: $\pm(x, y, z: {}^1/_2 - x; {}^1/_2 + y; {}^1/_2 - z)$ and $\pm(x, y, z; {}^1/_2 - x; {}^1/_2 + y; -z)$, respectively.

generate amine–hydride complexes;[14] this is shown for the generic case in eq 1. This particular transformation is of fundamental

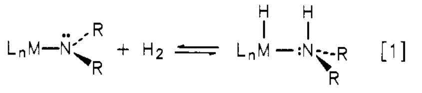

[1]

importance since it can be considered both as an example of the heterolytic cleavage of dihydrogen and as a hydrogenolysis of a metal–amide bond. In light of the potential significance of this reaction, we examined an extensive series of rhodium and iridium complexes containing the amine–hydride functionality, formed both from a starting amide complex and an amine derivative, all by quite different procedures and, presumably, different mechanisms. What became apparent was that the resulting similar stereochemistries of these complexes are dominated by the formation of an *inner-sphere* N–H···X hydrogen bond. In addition to stereochemical control, such hydrogen bonding appears to play an important role in the stabilization of these hydride complexes.

Experimental Section

Generation Information. All manipulations were performed under prepurified nitrogen in a Vacuum Atmospheres HE-553-2 glovebox equipped with an MO-40-2H purifier or in standard Schlenk-type glassware on a vacuum-line. Nitrogen and hydrogen gases were purified prior to use by passing the gases through columns of MnO on vermiculite and activated 4Å molecular sieves.[15] Both $RhCl_3\cdot xH_2O$ and $IrCl_3\cdot xH_2O$ were obtained from Johnson–Matthey and used as received to prepare $M(\eta^2\text{-}C_8H_{14})[N(SiMe_2CH_2PR_2)_2]$ and $M(CH_3)X[N(SiMe_2CH_2PR_2)_2]$ (M = Rh, Ir; R = Ph, *i*-Pr; X = I, Br), as outlined in a previous publication.[16]

Toluene and hexanes were distilled from $Na\text{-}Ph_2CO$ under argon. CH_2Cl_2 was refluxed over CaH_2 and vacuum-transferred prior to use. Deuteriated benzene (C_6D_6) was purchased from Aldrich, dried over activated 4Å molecular siieves, vacuum-transferred, and freeze/pump/thawed for several cycles.

Carbon, hydrogen, and nitrogen analyses of these air- and moisture-sensitive compounds were expertly performed by P. Borda of this department. Infrared spectra were recorded on either a Pye-Unicam SP-1100 or a Nicolet 5D-X as KBr disks or in solution. ^1H NMR spectra were run on a Bruker WH-400 (400 MHz), and NOE difference experiments were carried out on this instrument by using standard pulse sequences; $^{31}P\{^1H\}$ and $^{31}P\{^1H$ selectively decoupled$\}$ NMR spectra were recorded on a Bruker WP-80 at 32.442 MHz in 10-mm tubes and were referenced to external $P(OMe)_3$ at +141.0 ppm (relative to 85% H_3PO_4).

Dihydrogen Addition to $M(CH_3)X[N(SiMe_2CH_2PR_2)_2]$. $IrH(CH_3)I[NH(SiMe_2CH_2PR_2)_2]$. A solution of $Ir(CH_3)I[N(SiMe_2CH_2PR_2)_2]$ (~200 mg) in toluene (20 mL) was stirred under 1 atm H_2 at room temperature. Within minutes, the originally deep green (R = Ph) or blue-green (R = *i*-Pr) solution decolorized. After 1 h, the excess H_2 and solvent were removed in vacuo, and the resulting colorless oil crystallized from CH_2Cl_2/hexanes at −30 °C, yield 80–85%.

$IrH(CH_3)I[NH(SiMe_2CH_2PPh_2)_2]$. $^{31}P\{^1H\}$ NMR (C_6D_6) −1.82 (s); IR (CH_2Cl_2, cm^{-1}) ν_{Ir-H} = 2218 (m). Anal. Calcd for $C_{31}H_{41}IIrNP_2Si_2$: C, 43.05; H, 4.78; N, 1.62. Found: C, 42.70; H, 4.60; N, 1.60.

$IrH(CH_3)I[NH(SiMe_2CH_2P(i\text{-}Pr)_2)_2]$. $^{31}P\{^1H\}$ NMR (C_6D_6) −4.52 (s); $^{31}P\{^1H\}$ selectively decoupled −4.52 (d, $J_{H,P}$ = 14.4); IR (CH_2Cl_2, cm^{-1}) ν_{Ir-H} = 2238 (m). Anal. Calcd for $C_{19}H_{49}IIrNP_2Si_2$: C, 31.31; H, 6.78; N, 1.92. Found: C, 31.60; H, 6.86; N, 1.88.

$IrH_2I[NH(SiMe_2CH_2PR_2)_2]$. A solution of $Ir(CH_3)I[N$-

---

(14) Fryzuk, M. D.; MacNeil, P. A.; Rettig, S. J. *Organometallics* **1985**, *4*, 1145.

(15) Shriver, D. F. *The Manipulation of Air-Sensitive Compounds*; McGraw-Hill: New York, 1969; p 199.

(16) Fryzuk, M. D.; MacNeil, P. A.; Rettig, S. J. *Organometallics* **1986**, *5*, 2469.

Table IV. Final Positional (Fractional × 10^4; Ir, Rh, I, Cl, P, and Si × 10^5; H × 10^3) and Isotropic Thermal Parameters ($U \times 10^3$ Å^2)[a,b]

atom	*x*	*y*	*z*	U_{eq}/U_{iso}	atom	*x*	*y*	*z*	U_{eq}/U_{iso}
$Ir(CH_3)I(H)[NH(SiMe_2CH_2P(i\text{-}Pr)_2)_2]$									
Ir	43087 (2)	24091 (1)	36754 (2)	38	C(9)	1863 (7)	4982 (5)	1728 (9)	76
I	41321 (4)	41588 (3)	58055 (4)	57	C(10)	5265 (8)	1710 (5)	2 (7)	80
P(1)	20962 (13)	25285 (10)	25658 (14)	44	C(11)	5878 (7)	3695 (6)	593 (7)	70
P(2)	65627 (13)	20378 (10)	43147 (14)	45	C(12)	948 (8)	3225 (7)	4801 (9)	87
Si(1)	25750 (15)	37303 (12)	8863 (16)	51	C(13)	−408 (7)	3892 (6)	2528 (9)	88
Si(2)	55502 (14)	28342 (11)	14163 (15)	48	C(14)	2414 (8)	499 (5)	1452 (9)	86
N	4189 (4)	3370 (3)	2060 (5)	42	C(15)	133 (8)	1443 (6)	1195 (11)	98
C(1)	1699 (5)	2820 (5)	745 (6)	55	C(16)	7341 (9)	2304 (9)	7450 (8)	115
C(2)	6923 (5)	2620 (5)	3156 (6)	57	C(17)	8971 (7)	2408 (6)	6428 (7)	79
C(3)	4379 (6)	1585 (5)	5157 (7)	61	C(18)^1	6745 (20)	71 (11)	2885 (22)	224
C(4)	967 (6)	3494 (5)	3471 (7)	58	C(19)^2	8575 (19)	476 (13)	3446 (33)	230
C(5)	1571 (6)	1381 (5)	2177 (8)	68	C(20)^3	7356 (31)	127 (15)	4670 (56)	240
C(6)	7544 (6)	2534 (5)	6202 (6)	62	H(Ir)	452	145	234	63
C(7)	7460 (8)	731 (5)	4017 (10)	92	H(N)	446 (9)	373 (6)	263 (10)	121 (35)
C(8)	2466 (7)	3725 (7)	−1033 (8)	90					
$Rh(H)_2I[NH(SiMe_2CH_2P(i\text{-}Pr)_2)_2]$									
I	58352 (3)	12168 (1)	39396 (2)	59	C(9)	1393 (9)	1957 (3)	4035 (6)	128
Rh	38208 (3)	8884 (1)	20217 (2)	34	C(10)	−432 (6)	1554 (3)	1928 (6)	113
P(1)	40703 (10)	−1739 (5)	23244 (8)	40	C(11)	6872 (5)	−289 (3)	2505 (5)	80
P(2)	33674 (11)	19091 (5)	15071 (8)	40	C(12)	5991 (7)	−1130 (3)	3418 (6)	109
Si(1)	16126 (12)	1808 (6)	29776 (9)	50	C(13)	3707 (6)	−535 (3)	290 (4)	85
Si(2)	13873 (14)	16563 (7)	27677 (11)	64	C(14)	2933 (9)	−1320 (3)	1295 (6)	111
N	2275 (4)	942 (2)	2965 (3)	46	C(15)	6060 (5)	2221 (2)	1525 (4)	71
C(1)	3125 (4)	−354 (2)	3196 (3)	51	C(16)	4467 (5)	3127 (2)	1468 (5)	77
C(2)	2333 (5)	2244 (2)	2240 (3)	56	C(17)	3040 (6)	1801 (3)	−588 (4)	85
C(3)	5833 (5)	−468 (2)	3030 (4)	66	C(18)	875 (5)	1801 (3)	−174 (4)	77
C(4)	3234 (6)	−668 (2)	1159 (4)	73	H(Rh1)	277 (4)	69 (2)	94 (3)	43 (10)
C(5)	4852 (4)	2456 (2)	1828 (3)	51	H(Rh2)	471 (4)	81 (2)	132 (3)	73 (13)
C(6)	2341 (4)	2064 (2)	130 (3)	51	H(N)	300 (4)	99 (2)	347 (3)	48 (13)
C(7)	955 (5)	87 (3)	4071 (4)	75					
C(8)	197 (5)	7 (3)	1733 (4)	77					
$Ir(H)_2Cl[NH(SiMe_2CH_2PPh_2)_2]\cdot C_7H_8$									
Ir	40857 (1)	33213 (3)	58992 (2)	38	C(18)	5616 (3)	1761 (8)	7391 (6)	62
Cl	46834 (6)	35499 (16)	46233 (15)	52	C(19)	2885 (2)	4272 (7)	4949 (6)	46
P(1)	46555 (6)	26312 (17)	72157 (14)	43	C(20)	2731 (3)	3671 (8)	5782 (6)	57
P(2)	35054 (6)	41061 (17)	46430 (14)	41	C(21)	2266 (3)	3839 (10)	6013 (7)	77
Si(1)	45425 (8)	53236 (20)	77334 (17)	53	C(22)	1958 (3)	4617 (10)	5398 (9)	77
Si(2)	38760 (7)	64184 (17)	57725 (17)	48	C(23)	2108 (3)	5210 (9)	4563 (8)	74
N	4306 (2)	5344 (5)	6402 (5)	44	C(24)	2565 (3)	5035 (9)	4330 (6)	66
C(1)	4963 (3)	3984 (7)	7817 (6)	50	C(25)	3411 (2)	3368 (7)	3335 (5)	49
C(2)	3689 (2)	5713 (6)	4445 (6)	49	C(26)	3043 (3)	2544 (8)	3112 (7)	69
C(3)	4078 (3)	5051 (9)	8623 (6)	76	C(27)	2972 (4)	1968 (9)	2137 (8)	89
C(4)	4880 (3)	6775 (8)	8119 (7)	76	C(28)	3277 (4)	2137 (10)	1402 (7)	81
C(5)	3371 (3)	6602 (8)	6571 (7)	69	C(29)	3651 (4)	2925 (10)	1623 (6)	77
C(6)	4159 (3)	7965 (7)	5634 (7)	65	C(30)	3723 (3)	3566 (8)	2592 (6)	64
C(7)	4425 (3)	1759 (7)	8285 (6)	53	C(31)	2480 (8)	3018 (21)	9005 (14)	154
C(8)	4035 (4)	1006 (11)	8041 (8)	103	C(32)	2124 (7)	3123 (23)	9459 (14)	177
C(9)	3878 (4)	232 (13)	8784 (10)	131	C(33)	1718 (8)	2299 (28)	9612 (17)	196
C(10)	4108 (4)	232 (11)	9813 (8)	96	C(34)	1819 (15)	1282 (21)	9081 (20)	255
C(11)	4485 (4)	958 (10)	10070 (7)	89	C(35)	2195 (11)	981 (22)	8640 (17)	195
C(12)	4658 (4)	1702 (9)	9306 (6)	77	C(36)	2596 (11)	1630 (28)	8429 (14)	225
C(13)	5141 (2)	1560 (6)	6977 (5)	45	C(37)	2872 (7)	3583 (26)	8789 (15)	274
C(14)	5021 (3)	509 (7)	6414 (7)	68	H(Ir1)	369	317	674	82
C(15)	5361 (4)	−399 (8)	6298 (9)	89	H(Ir2)	380 (3)	205 (7)	552 (6)	91 (25)
C(16)	5819 (4)	−229 (9)	6742 (7)	75	H(N)	451 (2)	535 (6)	606 (5)	40 (22)
C(17)	5954 (3)	868 (11)	7273 (7)	79					

[a] esd's are in parentheses. [b] Superscripts refer to occupancy factors of 0.714, 0.776, and 0.510, respectively.

$(SiMe_2CH_2PR_2)_2]$ (~200 mg) in toluene (20 mL) was sealed in a 100-mL Pyrex reactor flask (with a Kontes needle-valve inlet) under 1 atm H_2 and heated at 80 °C for 2 days. The solution was then pumped down, and the colorless oily product crystallized from CH_2Cl_2/hexanes, yield 85–90%.

$IrH_2I[NH(SiMe_2CH_2PPh_2)_2]$. $^{31}P\{^1H\}$ NMR (C_6D_6) 6.97 (s); Ir (CH_2Cl_2, cm^{-1}) ν_{Ir-H} = 2218 (s, br). Anal. Calcd for $C_{30}H_{39}IIrNP_2Si_2$: C, 42.35; H, 4.62; N, 1.65. Found: C, 42.15; H, 4.38; N, 2.00.

$IrH_2I[NH(SiMe_2CH_2P(i\text{-}Pr)_2)_2]$. $^{31}P\{^1H\}$ NMR (C_6D_6) 2.46 (s); $^{31}P\{^1H$-selective$\}$ NMR 26.46 (t, J_H = 14.6); IR (CH_2Cl_2, cm^{-1}) ν_{Ir-H} = 2227 (s, br). Anal. Calcd for $C_{18}H_{47}IIrNP_2Si_2$: C, 30.24; H, 6.63; N, 1.96. Found: C, 30.44; H, 6.70; N, 1.90.

$IrH_2Br[NH(SiMe_2CH_2PPh_2)_2]$. This complex was prepared and purified as outlined for its iodo analogue, from $Ir(CH_3)Br[N(SiMe_2CH_2PPh_2)_2]$, except that heating at 80 °C under 1 atm H_2 was necessary for only 24 h, yield 87%. $^{31}P\{^1H\}$ NMR (C_6D_6) 8.55 (s); IR (CH_2Cl_2, cm^{-1}) ν_{Ir-H} = 2220 (s, br). Anal. Calcd. for $C_{30}H_{39}BrIrNP_2Si_2$: C, 44.82; H, 4.89; N, 1.74. Found: C, 44.79; H, 4.79; N, 1.69]. *Note*: Although the chloro dihydride, $IrH_2Cl[NH(SiMe_2CH_2PPh_2)_2]$, can be prepared in a similar fashion from either $Ir(CH_3)Cl[N(SiMe_2CH_2PPh_2)_2]$ or $Ir(CH_2Ph)Cl[N(SiMe_2CH_2PPh_2)_2]$,[17] the inherent difficulty in the preparation and/or purification of these two complexes makes this route rather inefficient. Alternatively, synthesis of the dihydrido chloride can be easily carried out by reaction of $Ir(\eta^2\text{-}C_8H_{14})[N(SiMe_2CH_2PPh_2)_2]$ with H_2 in CH_2Cl_2 (vide infra).

$RhH_2X[NH(SiMe_2CH_2PR_2)_2]$. A solution of $Rh(CH_3)X[N(SiMe_2CH_2PR_2)_2]$ (~200 mg) in toluene (20 mL) was stirred under 1 atm H_2 at room temperature. Complete decolorization of the originally

---

[17] Fryzuk, M. D.; MacNeil, P. A., unpublished results.

Table V. Bond Lengths (Å)[a]

bond	length (Å)	bond	length (Å)
$Ir(CH_3)I(H)[NH(SiMe_2CH_2P(i\text{-}Pr)_2)_2]$			
Ir–I	2.8176 (4)	Si(1)–C(9)	1.842 (7)
Ir–P(1)	2.3070 (13)	Si(2)–N	1.763 (5)
Ir–P(2)	2.3152 (14)	Si(2)–C(2)	1.861 (5)
Ir–N	2.368 (4)	Si(2)–C(10)	1.858 (7)
Ir–C(3)	2.127 (6)	Si(2)–C(11)	1.885 (6)
Ir–H(Ir)	1.65	N–H(N)	0.70 (8)
P(1)–C(1)	1.830 (6)	C(4)–C(12)	1.493 (10)
P(1)–C(4)	1.852 (6)	C(4)–C(13)	1.510 (9)
P(1)–C(5)	1.860 (6)	C(5)–C(14)	1.515 (10)
P(2)–C(2)	1.839 (6)	C(5)–C(15)	1.544 (10)
P(2)–C(6)	1.851 (6)	C(6)–C(16)	1.488 (10)
P(2)–C(7)	1.857 (7)	C(6)–C(17)	1.513 (9)
Si(1)–N	1.766 (5)	C(7)–C(18)	1.43 (2)
Si(1)–C(1)	1.862 (6)	C(7)–C(19)	1.48 (2)
Si(1)–C(8)	1.856 (7)	C(7)–C(20)	1.30 (2)
$Rh(H)_2I[NH(SiMe_2CH_2P(i\text{-}Pr)_2)_2]$			
I–Rh	2.8178 (4)	Si(1)–C(8)	1.859 (5)
Rh–P(1)	2.3004 (11)	Si(2)–N	1.747 (4)
Rh–P(2)	2.2854 (10)	Si(2)–C(2)	1.878 (5)
Rh–N	2.377 (3)	Si(2)–C(9)	1.854 (6)
Rh–H(Rh1)	1.56 (3)	Si(2)–C(10)	1.839 (6)
Rh–H(Rh2)	1.56 (4)	N–H(N)	0.83 (4)
P(1)–C(1)	1.826 (4)	C(3)–C(11)	1.531 (7)
P(1)–C(3)	1.845 (4)	C(3)–C(12)	1.497 (8)
P(1)–C(4)	1.859 (5)	C(4)–C(13)	1.464 (7)
P(2)–C(2)	1.843 (4)	C(4)–C(14)	1.452 (7)
P(2)–C(5)	1.849 (4)	C(5)–C(15)	1.525 (6)
P(2)–C(6)	1.849 (4)	C(5)–C(16)	1.520 (6)
Si(1)–N	1.763 (4)	C(6)–C(17)	1.517 (7)
Si(1)–C(1)	1.868 (4)	C(6)–C(18)	1.525 (7)
Si(1)–C(7)	1.860 (5)		
$Ir(H)_2Cl[NH(SiMe_2CH_2PPh_2)_2]\cdot C_7H_8$			
Ir–Cl	2.487 (2)	C(11)–C(12)	1.393 (12)
Ir–P(1)	2.287 (2)	C(13)–C(14)	1.363 (10)
Ir–P(2)	2.293 (2)	C(13)–C(18)	1.386 (9)
Ir–N	2.340 (6)	C(14)–C(15)	1.390 (11)
Ir–H(Ir1)	1.64	C(15)–C(16)	1.348 (13)
Ir–H(Ir2)	1.64 (8)	C(16)–C(17)	1.393 (13)
P(1)–C(1)	1.818 (7)	C(17)–C(18)	1.374 (12)
P(1)–C(7)	1.836 (8)	C(19)–C(20)	1.358 (10)
P(1)–C(13)	1.843 (7)	C(19)–C(24)	1.389 (10)
P(2)–C(2)	1.839 (7)	C(20)–C(21)	1.384 (11)
P(2)–C(19)	1.839 (7)	C(21)–C(22)	1.376 (13)
P(2)–C(25)	1.831 (7)	C(22)–C(23)	1.351 (12)
Si(1)–N	1.736 (6)	C(23)–C(24)	1.366 (11)
Si(1)–C(1)	1.864 (8)	C(25)–C(26)	1.367 (11)
Si(1)–C(3)	1.854 (8)	C(25)–C(30)	1.383 (10)
Si(1)–C(4)	1.867 (8)	C(26)–C(27)	1.378 (12)
Si(2)–N	1.790 (6)	C(27)–C(28)	1.356 (13)
Si(2)–C(2)	1.865 (8)	C(28)–C(29)	1.355 (13)
Si(2)–C(5)	1.856 (7)	C(29)–C(30)	1.404 (11)
Si(2)–C(6)	1.870 (8)	C(31)–C(32)	1.22 (2)
N–H(N)	0.76 (6)	C(31)–C(36)	1.72 (3)
C(7)–C(8)	1.370 (11)	C(31)–C(37)	1.32 (2)
C(7)–C(12)	1.378 (10)	C(32)–C(33)	1.48 (3)
C(8)–C(9)	1.375 (13)	C(33)–C(34)	1.34 (3)
C(9)–C(10)	1.382 (14)	C(34)–C(35)	1.30 (4)
C(10)–C(11)	1.325 (13)	C(35)–C(36)	1.38 (3)

[a] esd's are in parentheses.

blue-green solution of $Rh(CH_3)I[N(SiMe_2CH_2PPh_2)_2]$ occurred within 1 h under these conditions whereas its deep purple isopropyl analogue, $Rh(CH_3)I[N(SiMe_2CH_2P(i\text{-}Pr)_2)_2]$, required 3 h to fully react with H_2. The bromo analogue requires 4 days for complete reaction under ambient conditions. After solvent removal, crystallization from CH_2Cl_2/hexanes resulted in colorless or off-white crystals, yield 80–90%.

$RhH_2I[NH(SiMe_2CH_2PPh_2)_2]$. $^{31}P\{^1H\}$ NMR (C_6D_6) 32.07 (d, $^1J_{Rh}$ = 114.8); Ir (CH_2Cl_2, cm^{-1}) ν_{Rh-H} = 2063 (s, br). Anal. Calcd for $C_{30}H_{39}INP_2RhSi_2$: C, 47.31; H, 5.16; N, 1.84. Found: C, 47.11; H, 5.16; N, 2.00.

$RhH_2I[NH(SiMe_2CH_2P(i\text{-}Pr)_2)_2]$. $^{31}P\{^1H\}$ NMR (C_6D_6) 51.30 (d. $^1J_{Rh}$ = 107.4); $^{31}P\{^1H\}$ selectively decoupled 51.30 (dt, $^1J_{Rh}$ = 107.4, ^2J_H = 12.5); Ir (CH_2Cl_2, cm^{-1}) ν_{Rh-H} = 2080 (s, br). Anal. Calcd for $C_{18}H_{47}INP_2RhSi_2$: C, 34.56; H, 7.57; N, 2.24. Found: C, 34.29; H, 7.30; N, 2.40.

$RhH_2Br[NH(SiMe_2CH_2PPh_2)_2]$. $^{31}P\{^1H\}$ NMR (C_6D_6) 32.39 (d, $^1J_{Rh}$ = 114.8); IR (CH_2Cl_2, cm^{-1}) ν_{Rh-H} = 2068 (s, br). Anal. Calcd for $C_{30}H_{39}BrNP_2RhSi_2$: C, 50.42; H, 5.50; N, 1.96. Found: C, 50.16; H, 5.55; N, 1.96.

Reaction of $M(\eta^2\text{-}C_8H_{14})[N(SiMe_2CH_2PPh_2)_2]$ with H_2 in the Presence of CH_2X_2. The following synthesis is for the chloro derivatives, $MH_2Cl[NH(SiMe_2CH_2PPh_2)_2]$, although the bromo and iodo derivatives can be prepared in an identical fashion. However, since isolation of these latter species is complicated by further reaction to form small amounts of $MX_2H[NH(SiMe_2CH_2PPh_2)_2]$ (X = Br, I), these complexes are more conveniently prepared as described above.

A solution of $M(\eta^2\text{-}C_8H_{14})[N(SiMe_2CH_2PPh_2)_2]$ (~200 mg) in CH_2Cl_2 (20 mL) was stirred under 1 atm H_2 at room temperature. The orange-colored solution gradually lightened to a bright yellow (~1 h); over the course of an additional 24-h period, the solution decolorized. Following solvent removal and crystallization from CH_2Cl_2/hexanes, large colorless blocks of the dihydrido chloride complex were obtained.

$IrH_2Cl[NH(SiMe_2CH_2PPh_2)_2]$. $^{31}P\{^1H\}$ NMR (C_6D_6) 8.85 (s); IR (CH_2Cl_2, cm^{-1}) ν_{Ir-H} = 2177 (s, br). Anal. Calcd for $C_{30}H_{39}ClIrNP_2Si_2$: C, 47.45; H, 5.18; N, 1.84. Found: C, 47.18; H, 5.04; N, 1.70.

$RhH_2Cl[NH(SiMe_2CH_2PPh_2)_2]$. $^{31}P\{^1H\}$ NMR (C_6D_6) 31.84 (d, $^1J_{Rh}$ = 114.8); IR (CH_2Cl_2, cm^{-1}) ν_{Rh-H} = 2065 (s, br). Anal. Calcd for $C_{30}H_{39}ClNP_2RhSi_2$: C, 53.73; H, 5.86; N, 2.09. Found: C, 53.44; H, 5.94; N, 2.20.

Dihydrogen Addition to the M(I) Amine Chlorides. $Ir(1,5\text{-}COD)Cl[NH(SiMe_2CH_2PPh_2)_2]$. To a solution of $\{Ir(1,5\text{-}COD)Cl\}_2$ (170 mg, 0.25 mmol) in toluene (50 mL) was slowly added a solution of the amine, $NH(SiMe_2CH_2PPh_2)_2$[18] (260 mg, 0.50 mmol), in toluene (10 mL). Immediately, the orange color of the iridium starting material faded to a deep yellow. The clear solution was pumped down, and the oily product was crystallized from toluenes/hexanes to give yellow crystals of the iridium(I) amine chloride. $^{31}P\{^1H\}$ NMR (C_6D_6) −17.03 (s, br); ^1H NMR (C_6D_6) $Si(CH_3)_2$, −0.09 (s. br); $P(C_6H_5)_2$, 7.14 (m, para/meta), 7.63 (m, ortho); = CH (of 1,5-COD), 3.6 (m, v br); CH_2P, CH_2 (of 1,5-COD) and NH, 1.5→2.5 (v br, undefined). Anal. Calcd for $C_{38}H_{49}ClIrNP_2Si_2$: C, 52.73; H, 5.70; N, 1.62. Found: C, 53.00; H, 5.90; N, 1.50.

Exposure of the above complex (~100 mg) in toluene (10 mL) to 1 atm H_2 at room temperature resulted in rapid decolorization. After 1 h, the solvent was removed in vacuo, and the product was isolated as previously described.

$\{RhCl[NH(SiMe_2CH_2PPh_2)_2]\}_n$. A solution of the amine, $NH(SiMe_2CH_2PPh_2)_2$ (260 mg, 0.50 mmol), in toluene (10 mL) was added to a solution of $\{Rh(\eta^2\text{-}C_8H_{14})_2Cl\}_2$ (179 mg, 0.25 mmol) in toluene (50 mL). The solution deepened to a clear dark red color. Stirring was continued overnight, whereupon the solvent was removed; the product crystallized as small red clusters form toluene/hexanes. $^{31}P\{^1H\}$ NMR (C_6D_6) 35.56 (d, $^1J_{Rh}$ = 192.88); ^1H NMR (C_6D_6) $Si(CH_3)_2$, 0.36(s); CH_2P, 1.23 (m, br); NH, 2.68 (s, br); $P(C_6H_5)_2$, 7.02 (m, para/meta), 7.77 (m, ortho). Anal. Calcd for $C_{30}H_{38}ClNP_2RhSi_2\cdot 0.5C_7H_8$: C, 56.34; H, 5.79; N, 1.96. Found: C, 56.88; H, 6.04; N, 1.65.

Conversion of the above complex to its Rh(III) dihydride derivative was carried out in a identical manner as described above for $Ir(1,5\text{-}COD)Cl[NH(SiMe_2CH_2PPh_2)_2]$. Isolation of $RhH_2Cl[NH(SiMe_2CH_2PPh_2)_2]$ was as previously outlined, yield 92%.

Deuteriation Studies. The reactions to generate the corresponding deuterides were carried out exactly as described above for the hydrides by using D_2 (Matheson, 99.5% enriched).

X-ray Crystallographic Analyses. Crystallographic data for $IrH(CH_3)I[NH(SiMe_2CH_2P(i\text{-}Pr)_2]$, $RhH_2I[NH(SiMe_2CH_2P(i\text{-}Pr)_2)_2]$, and $IrH_2Cl[NH(SiMe_2CH_2PPh_2)_2]\cdot CH_3C_6H_5$ are presented in Table III. Final unit-cell parameters were obtained by least-squares on $2\sin\theta/\lambda$ values for 25 reflections (with 2θ = 30–43°) measured with Mo $K\alpha_1$ radiation. The data were corrected for absorption[19-21] and, where appropriate, for linear decay.

All three structures were solved by conventional heavy-atom methods, the coordinates of metal, halogen, P, and Si atoms being determined from the Patterson functions. In the case of the triclinic structure, the centrosymmetric space group $P\bar{1}$ was indicated by the Patterson function and was verified by the structure analysis. All remaining atoms, including amine and metal hydrogen atoms, were positioned from subsequent difference maps. In the final stages of refinement all non-hydrogen atoms were refined with anisotropic thermal parameters. All amine hydrogen atoms and three of the five metal hydrogen atoms were refined with isotropic thermal parameters. For each of the Ir complexes refinement of hydride positions was hampered by proximity to large residual peaks

---

[18] Fryzuk, M. D.; MacNeil, P. A.; Rettig, S. J.; Secco, A. S.; Trotter, J. *Organometallics* **1982**, *1*, 918.

Table VI. Bond Angles (deg)

bonds	angle (deg)	bonds	angle (deg)	bonds	angle (deg)	bonds	angle (deg)
$Ir(CH_3)I(H)[NH(SiMe_2CH_2P(i\text{-}Pr)_2)_2]$							
I–Ir–P(1)	97.29 (3)	C(1)–Si(1)–C(9)	113.0 (3)	Ir–P(1)–C(4)	118.0 (2)	P(1)–C(4)–C(12)	111.6 (5)
I–Ir–P(2)	94.88 (4)	C(8)–Si(1)–C(9)	108.8 (4)	Ir–P(1)–C(5)	115.5 (2)	P(1)–C(4)–C(13)	119.0 (5)
I–Ir–N	86.59 (11)	N–Si(2)–C(2)	102.6 (2)	C(1)–P(1)–C(4)	105.6 (3)	C(12)–C(4)–C(13)	110.4 (6)
I–Ir–C(3)	91.9 (2)	N–Si(2)–C(10)	108.9 (3)	C(1)–P(1)–C(5)	105.5 (3)	P(1)–C(5)–C(14)	112.8 (4)
I–Ir–H(Ir)	172	N–Si(2)–C(11)	112.5 (3)	C(4)–P(1)–C(5)	105.5 (3)	P(1)–C(5)–C(15)	113.7 (5)
P(1)–Ir–P(2)	167.30 (5)	C(2)–Si(2)–C(10)	115.0 (3)	Ir–P(2)–C(2)	106.2 (2)	C(14)–C(5)–C(15)	107.9 (6)
P(1)–Ir–N	88.72 (11)	C(2)–Si(2)–C(11)	108.0 (3)	Ir–P(2)–C(6)	119.9 (2)	P(2)–C(6)–C(16)	115.6 (5)
P(1)–Ir–C(3)	90.5 (2)	C(10)–Si(2)–C(11)	109.7 (3)	Ir–P(2)–C(7)	118.6 (3)	P(2)–C(6)–C(17)	115.9 (5)
P(1)–Ir–H(Ir)	87	Ir–N–Si(1)	111.6 (2)	C(2)–P(2)–C(6)	101.5 (3)	C(16)–C(6)–C(17)	112.6 (6)
P(2)–Ir–N	88.37 (11)	Ir–N–Si(2)	107.5 (2)	C(2)–P(2)–C(7)	105.8 (4)	P(2)–C(7)–C(18)	116.4 (7)
P(2)–Ir–C(3)	92.7 (2)	Ir–N–H(N)	95 (8)	C(6)–P(2)–C(7)	102.7 (4)	P(2)–C(7)–C(19)	117.8 (10)
P(2)–Ir–H(Ir)	81	Si(1)–N–Si(2)	123.6 (3)	N–Si(1)–C(1)	106.8 (2)	P(2)–C(7)–C(20)	119.7 (13)
N–Ir–C(3)	178.2 (2)	Si(1)–N–H(N)	118 (7)	N–Si(1)–C(8)	113.8 (3)	C(18)–C(7)–C(19)	97.0 (15)
N–Ir–H(Ir)	86	Si(2)–N–H(N)	96 (8)	N–Si(1)–C(9)	107.5 (3)	C(18)–C(7)–C(20)	73 (2)
C(3)–Ir–H(Ir)	95	P(1)–C(1)–S(1)	110.8 (3)	C(1)–Si(1)–C(8)	107.1 (3)	C(19)–C(7)–C(20)	119.7 (15)
Ir–P(1)–C(1)	105.5 (2)	P(2)–C(2)–Si(2)	112.9 (3)				
$Rh(H)_2I[NH(SiMe_2CH_2P(i\text{-}Pr)_2)_2]$							
I–Rh–P(1)	94.34 (3)	C(1)–Si(1)–C(7)	108.7 (2)	Rh–P(1)–C(1)	105.93 (14)	P(1)–C(1)–Si(1)	111.7 (2)
I–Rh–P(2)	93.31 (3)	C(1)–Si(1)–C(8)	111.6 (2)	Rh–P(1)–C(3)	117.2 (2)	P(2)–C(2)–Si(2)	115.3 (2)
I–Rh–N	83.81 (9)	C(7)–Si(1)–C(8)	109.5 (2)	Rh–P(1)–C(4)	114.3 (2)	P(1)–C(3)–C(11)	112.7 (4)
I–Rh–H(Rh1)	176.8 (13)	N–Si(2)–C(2)	109.1 (2)	C(1)–P(1)–C(3)	103.5 (2)	P(1)–C(3)–C(12)	118.2 (4)
I–Rh–H(Rh2)	102 (2)	N–Si(2)–C(9)	108.9 (3)	C(1)–P(1)–C(4)	104.6 (2)	C(11)–C(3)–C(12)	113.4 (5)
P(1)–Rh–P(2)	172.33 (4)	N–Si(2)–C(10)	111.0 (3)	C(3)–P(1)–C(4)	109.7 (2)	P(1)–C(4)–C(13)	114.1 (4)
P(1)–Rh–N	90.16 (9)	C(2)–Si(2)–C(9)	107.4 (3)	Rh–P(2)–C(2)	107.09 (15)	P(1)–C(4)–C(14)	119.1 (4)
P(1)–Rh–H(Rh1)	84.5 (13)	C(2)–Si(2)–C(10)	112.8 (2)	Rh–P(2)–C(5)	117.60 (14)	C(13)–C(4)–C(14)	115.8 (5)
P(1)–Rh–H(Rh2)	87 (2)	C(9)–Si(2)–C(10)	107.5 (4)	Rh–P(2)–C(6)	118.02 (14)	P(2)–C(5)–C(15)	114.3 (3)
P(2)–Rh–N	91.11 (9)	Rh–N–Si(1)	107.2 (2)	C(2)–P(2)–C(5)	102.2 (2)	P(2)–C(5)–C(16)	114.5 (3)
P(2)–Rh–H(Rh1)	87.8 (13)	Rh–N–Si(2)	111.7 (2)	C(2)–P(2)–C(6)	104.9 (2)	C(15)–C(5)–C(16)	111.4 (4)
P(2)–Rh–H(Rh2)	91 (2)	Rh–N–H(N)	83 (3)	C(5)–P(2)–C(6)	105.2 (2)	P(2)–C(6)–C(17)	111.6 (3)
N–Rh–H(Rh1)	99.1 (12)	Si(1)–N–Si(2)	128.4 (2)	N–Si(1)–C(1)	105.1 (2)	P(2)–C(6)–C(18)	112.0 (3)
N–Rh–H(Rh2)	174 (2)	Si(1)–N–H(N)	110 (3)	N–Si(1)–C(7)	111.0 (2)	C(17)–C(6)–C(18)	109.5 (4)
H(Rh1)–Rh–H(Rh2)	75 (2)	Si(2)–N–H(N)	107 (3)	N–Si(1)–C(8)	110.9 (2)		
$Ir(H)_2Cl[NH(SiMe_2CH_2PPh_2)_2]\cdot C_7H_8$							
Cl–Ir–P(1)	92.39 (6)	Si(2)–N–H(N)	105 (5)	Ir–P(2)–C(19)	119.8 (2)	C(19)–C(20)–C(21)	120.3 (8)
Cl–Ir–P(2)	89.34 (6)	P(1)–C(1)–Si(1)	109.7 (4)	Ir–P(2)–C(25)	118.5 (2)	C(20)–C(21)–C(22)	120.1 (8)
Cl–Ir–N	84.7 (2)	P(2)–C(2)–Si(2)	108.4 (4)	C(2)–P(2)–C(19)	103.0 (3)	C(21)–C(22)–C(23)	120.0 (8)
Cl–Ir–H(Ir1)	180	P(1)–C(7)–C(8)	119.0 (6)	C(2)–P(2)–C(25)	107.4 (3)	C(22)–C(23)–C(24)	119.8 (8)
Cl–Ir–H(Ir2)	104 (2)	P(1)–C(7)–C(12)	123.4 (6)	C(19)–P(2)–C(25)	101.7 (3)	C(19)–C(24)–C(23)	121.2 (8)
P(1)–Ir–P(2)	176.66 (7)	C(8)–C(7)–C(12)	117.1 (8)	N–Si(1)–C(1)	103.1 (3)	P(2)–C(25)–C(26)	119.4 (6)
P(1)–Ir–N	88.25 (15)	C(7)–C(8)–C(9)	121.6 (9)	N–Si(1)–C(3)	112.6 (4)	P(2)–C(25)–C(30)	121.3 (6)
P(1)–Ir–H(Ir1)	87.6	C(8)–C(9)–C(10)	119.8 (10)	N–Si(1)–C(4)	111.3 (4)	C(26)–C(25)–C(30)	119.1 (7)
P(1)–Ir–H(Ir2)	102 (3)	C(9)–C(10)–C(11)	119.7 (9)	C(1)–Si(1)–C(3)	109.3 (4)	C(25)–C(26)–C(27)	120.1 (8)
P(2)–Ir–N	89.06 (15)	C(10)–C(11)–C(12)	120.6 (9)	C(1)–Si(1)–C(4)	110.0 (4)	C(26)–C(27)–C(28)	121.6 (9)
P(2)–Ir–H(Ir1)	90.7	C(7)–C(12)–C(11)	121.0 (8)	C(3)–Si(1)–C(4)	110.3 (4)	C(27)–C(28)–C(29)	118.9 (8)
P(2)–Ir–H(Ir2)	80 (3)	P(1)–C(13)–C(14)	118.1 (5)	N–Si(2)–C(2)	103.6 (3)	C(28)–C(29)–C(30)	120.9 (8)
N–Ir–H(Ir1)	95.3	P(1)–C(13)–C(18)	122.4 (6)	N–Si(2)–C(5)	110.1 (4)	C(25)–C(30)–C(29)	119.2 (8)
N–Ir–H(Ir2)	166 (3)	C(14)–C(13)–C(18)	119.4 (7)	N–Si(2)–C(6)	110.6 (3)	C(32)–C(31)–C(36)	120 (2)
H(Ir1)–Ir–H(Ir2)	76	C(13)–C(14)–C(15)	121.2 (8)	C(2)–Si(2)–C(5)	113.0 (3)	C(32)–C(31)–C(37)	144 (3)
Ir–P(1)–C(1)	107.2 (3)	C(14)–C(15)–C(16)	119.3 (9)	C(2)–Si(2)–C(6)	110.9 (3)	C(36)–C(31)–C(37)	96 (2)
Ir–P(1)–C(7)	115.4 (2)	C(15)–C(16)–C(17)	120.3 (8)	C(5)–Si(2)–C(6)	108.6 (4)	C(31)–C(32)–C(33)	134 (3)
Ir–P(1)–C(13)	123.3 (2)	C(16)–C(17)–C(18)	120.2 (8)	Ir–N–Si(1)	108.0 (3)	C(32)–C(33)–C(34)	102 (2)
C(1)–P(1)–C(7)	107.2 (3)	C(13)–C(18)–C(17)	119.4 (8)	Ir–N–Si(2)	110.2 (3)	C(33)–C(34)–C(35)	131 (4)
C(1)–P(1)–C(13)	104.6 (3)	P(2)–C(19)–C(20)	121.4 (6)	Ir–N–H(N)	93 (5)	C(34)–C(35)–C(36)	133 (3)
C(7)–P(1)–C(13)	97.8 (3)	P(2)–C(19)–C(24)	120.1 (6)	Si(1)–N–Si(2)	126.6 (4)	C(31)–C(36)–C(35)	99 (2)
Ir–P(2)–C(2)	105.0 (2)	C(20)–C(19)–C(24)	118.5 (7)	Si(1)–N–H(N)	109 (5)		

[a] esd's are in parentheses.

near the metal. These hydrogen atoms were kept fixed in the observed positions. The remaining hydrogen atoms were fixed in idealized positions (based on observed positions for methyl groups, $C(sp^3)-H = 0.98$, $C(sp^2)-H = 0.97$ Å). In the case of $IrH(CH_3)I[NH(SiMe_2CH_2P(i\text{-}Pr)_2]$ one of the isopropyl groups was found to be disordered, the two methyl carbon atoms occupying three positions. The occupancy factors were initially estimated from relative peak heights on a Fourier map and were subsequently adjusted to result in nearly equal thermal parameters. Neutral atom scattering factors for all atoms and anomalous scattering corrections for Ir, Rh, I, Cl, P, and Si atoms were taken from ref 22.

Final atomic coordinates and equivalent isotropic ($U_{eq} = {}^1/_3$ trace diagonalized U) or isotropic thermal parameters are given in Table IV. Bond lengths, bond angles, and intra-annular torsion angles appear in Tables V–VII. Calculated hydrogen parameters, anisotropic thermal parameters, torsion angles, measured and calculated structure factor amplitudes, and intramolecular X···H interactions (Tables S1–S7) are included as Supplementary Material.

Notes on Structures. Intermolecular distances in all three structures generally correspond to normal van der Waals contacts. In each case there are weak H···X interactions of possible significance. Molecules of $IrH(CH_3)I[NH(SiMe_2CH_2P(i\text{-}Pr)_2)_2]$ form weakly associated centrosymmetric dimers via the interaction C(11)–H(11b)···I($1 - x$, $1 - y$, $1 - z$) [H···I = 3.10, C···I = 4.018 (7) Å, C–H···I = 156°]. In the structure of $RhH_2I[NH(SiMe_2CH_2P(i\text{-}Pr)_2)_2]$, infinite chains result from the interaction C(6)–H(6)···I($x - {}^1/_2$, ${}^1/_2 - y$, $z - {}^1/_2$) [H···I = 3.19, C···I = 4.092 (4) Å, C–H···I = 155°]. The interactions in $IrH_2Cl[NH(SiMe_2CH_2PPh_2)_2]$ are more extensive and include a weak N–H···Cl hydrogen bond. The complex molecules form centrosymmetric dimers via a pair of interactions [N–H(N)···Cl ($1 - x$, $1 - y$, $1 - z$), H···Cl = 2.79 (6), N···Cl = 3.479 (7) Å, N–H···Cl = 152 (6)°; C(6)–H(6a)···Cl(1

Table VII. Intra-Annular Torsion Angles (deg)[a]

atoms	value (deg)
$Ir(CH_3)I(H)[NH(SiMe_2CH_2P(i\text{-}Pr)_2)_2]$	
N-Ir-P(1)-C(1)	21.7 (2)
Ir-P(1)-C(1)-Si(1)	-41.1 (3)
N-Si(1)-C(1)-P(1)	43.0 (4)
C(1)-Si(1)-N-Ir	-24.1 (3)
P(1)-Ir-N-Si(1)	1.6 (2)
N-Ir-P(2)-C(2)	-3.3 (2)
Ir-P(2)-C(2)-Si(2)	-23.9 (4)
N-Si(2)-C(2)-P(2)	47.3 (4)
C(2)-Si(2)-N-Ir	-47.1 (3)
P(2)-Ir-N-Si(2)	30.7 (2)
$Rh(H)_2I[NH(SiMe_2CH_2P(i\text{-}Pr)_2)_2]$	
N-Rh-P(1)-C(1)	-5.6 (2)
Rh-P(1)-C(1)-Si(1)	31.0 (2)
N-Si(1)-C(1)-P(1)	-48.7 (3)
C(1)-Si(1)-N-Rh	41.0 (2)
P(1)-Rh-N-Si(1)	-21.4 (2)
N-Rh-P(2)-C(2)	8.9 (2)
Rh-P(2)-C(2)-Si(2)	-21.8 (3)
N-Si(2)-C(2)-P(2)	26.8 (3)
C(2)-Si(2)-N-Rh	-18.3 (3)
P(2)-Rh-N-Si(2)	5.7 (2)
$Ir(H)_2Cl[NH(SiMe_2CH_2PPh_2)_2]\cdot C_7H_8$	
N-Ir-P(1)-C(1)	-3.2 (3)
Ir-P(1)-C(1)-Si(1)	30.5 (4)
N-Si(1)-C(1)-P(1)	-50.9 (4)
C(1)-Si(1)-N-Ir	46.5 (4)
P(1)-Ir-N-Si(1)	-26.3 (3)
N-Ir-P(2)-C(2)	19.4 (3)
Ir-P(2)-C(2)-Si(2)	-44.6 (3)
N-Si(2)-C(2)-P(2)	52.2 (4)
C(2)-Si(2)-N-Ir	-35.2 (4)
P(2)-Ir-N-Si(2)	9.7 (3)

[a] esd's are in parentheses.

$-x, 1-y, 1-z$), H···Cl = 2.92, C···Cl = 3.689 (8) Å, C-H···Cl = 136°]. These dimers are linked by C(15)-H(15)···Cl ($1-x, 1-y, 1-z$) interactions [H···Cl = 2.69, C···Cl = 3.601 (9) Å, C-H···Cl = 156°] to form infinite arrays extending along the *b* axis. The solvent molecules are well separated from the complex molecules and from one another.

High thermal motion and/or unresolved minor disordering results in anomalous geometrical parameters for the solvent molecule [C(31)-C(37)] in the structure of $IrH_2Cl[NH(SiMe_2CH_2PPh_2)_2]\cdot C_7H_8$.

Results and Discussion

Other work from our laboratory[16,23] has established that the formally 16-electron methyl-halide complexes $M(CH_3)X[N(SiMe_2CH_2PR_2)_2]$ (M = Rh, Ir; X = Br, I; R = Ph, *i*-Pr) are square-pyramidal, both in the solid state and in solution, with the methyl group apical. All of these derivatives **1–4** react with dihydrogen to generate octahedral amine–hydride complexes with remarkably similar stereochemistries.

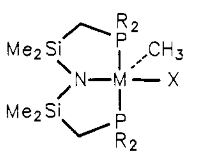

	M	X	R
1a	Ir	I	Ph
1b	Ir	I	Pr^i
2a	Rh	I	Ph
2b	Rh	I	Pr^i
3	Ir	Br	Ph
4	Rh	Br	Ph

For the iridium methyl iodide derivatives **1a** and **1b**, the major product (>90% by ^1H NMR) is the amine–monohydride complex **5** (**a**,**b**), with minor, but detectable, amounts of the corresponding amine–dihydride derivatives **6**(**a**,**b**) also formed (eq 2). The configuration of these complexes has been determined in the solid state (X-ray crystallography of **5b**), and the stereochemistry was confirmed in solution by ^1H NMR nuclear Overhauser difference experiments (NOEDIFF).[24] Most notable is that the major products **5**(**a**,**b**) have the methyl group cis to the hydride and the amine ligand cis to the iodide; from the X-ray crystal structure of **5b**, as shown in Figure 1, the syn relationship of the N–H and Ir–I bonds is apparent. None of the other possible stereoisomers have been detected for either of the products described above. Exclusive formation of the amine–dihydrides **6**(**a**,**b**) can be accomplished by heating both the methyl–iodide staring material at 80 °C under 1 atm H_2 for 24 h (eq 3) or by heating the intermediate amine–monohydride with additional H_2 overnight.

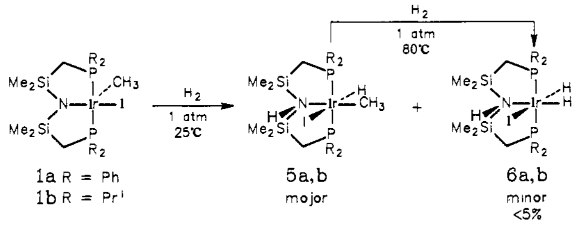

[2]

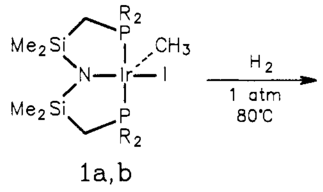

6a R = Ph
6b R = Pr^i [3]

Similarly, the iridium methyl bromide **3** reacts with dihydrogen to produce a nearly 1:1 mixture of the amine–monohydride, $IrH(CH_3)Br[NH(SiMe_2CH_2PPh_2)_2]$,[25] and the amine–dihydride, $IrH_2Br[NH(SiMe_2CH_2PPh_2)_2]$ (eq 4); once again, gentle heating of the reaction mixture with additional dihydrogen results in total conversion to the amine–dihydride.

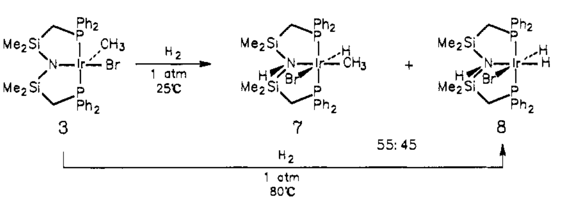

[4]

The corresponding reactions utilizing the methyl chloride complexes of iridium were not investigated because of the difficulty[16] in preparing pure samples of these starting complexes.

Under identical conditions, exposure of the analogous rhodium methyl halides **2a**, **2b**, and **4** results *only* in dihydride formation (eq 5). Monitoring this reaction in a sealed NMR tube by ^1H NMR indicates only the presence of amine–dihydride and starting material at any time.

In addition to solution spectroscopic data (see Tables I and II and Experimental Section), **9b** was subjected to an X-ray crystallographic determination (Figure 2). Several similarities can be immediately noticed between the aforementioned iridium amine–monohydride **5b** and the rhodium amine–dihydride **9b**; in particular, reaction with dihydrogen has resulted in apparent

---

(19) The computer programs used include locally written programs for data processing and locally modified versions of the following: ORFLS, full-matrix least-squares, and ORFFE, function and errors, by W. R. Busing, K. O. Martin, and H. A. Levy; FORDAP, Patterson and Fourier syntheses, by A. Zalkin; ORTEPII, illustrations, by C. K. Johnson.

(20) Coppens, P.; Leiserowitz, L.; Rabinovich, D. *Acta Crystallogr.* **1965**, *18*, 1035–1038.

(21) De Meulenaer, J.; Tompa, H. *Acta Crystallogr.* **1965**, *19*, 1014–1018.

(22) *International Tables for X-ray Crystallography*; Kynoch Press: Birmingham, England, 1974; Vol. IV.

(23) Fryzuk, M. D.; MacNeil, P. A.; Ball, R. G. *J. Am. Chem. Soc.* **1986**, *108*, 6414.

(24) Easton, J. W.; Saunders, J. K. *The Nuclear Overhauser Effect, Determination of Organic Structure by Physical Methods*; Nachad, F. C., Zuckerman, J. J., Randall, E. W., Eds.; Academic Press: New York, 1976; Vol. 6, p 271.

(25) Due to contamination by the amine-dihydride complex **8**, the amine-monohydride species was not obtainable in analytically pure form.

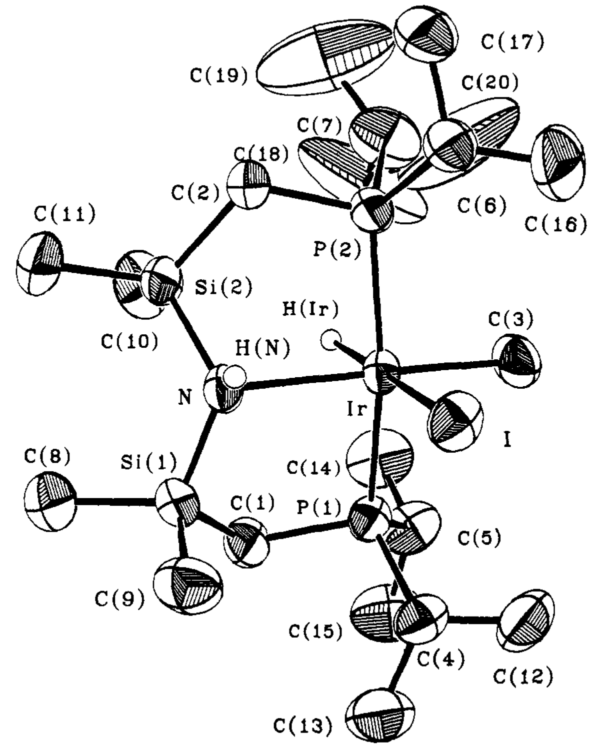

Figure 1. Molecular structure and numbering scheme for $IrH(CH_3)I[NH(SiMe_2CH_2P(i\text{-}Pr)_2)_2]$, **5b**.

protonation of the amide functionality to give a coordinated amine, and the N–H unit is, as before, syn to the metal–halogen bond.

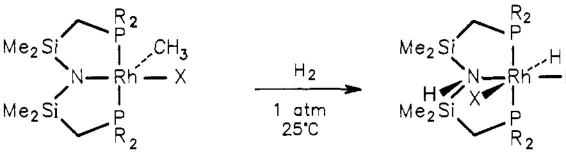

[5]

2a,b
4

	R	X
9a	Ph	I
9b	Pr^i	I
10	Ph	Br

The rhodium and iridium amine–dihydrides can also be formed by a completely different route. Exposure of a toluene solution of the iridium(I) or rhodium(I) cyclooctene amides **11** and **12** to dihydrogen in the presence of excess methylene dihalide, CH_2X_2 ($X = Cl, Br, I$), results in conversion to the amine–dihydrides, $MH_2X[NH(SiMe_2CH_2PPh_2)_2]$ ($M = Ir$; $X = I, Br, Cl$; $M = Rh$; $X = Cl$) (eq 6). Since this reaction is rather slow, requiring 24

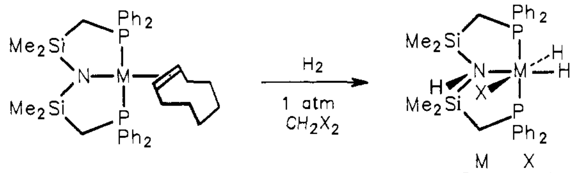

[6]

11 M = Ir
12 M = Rh

	M	X
6a	Ir	I
8	Ir	Br
13	Ir	Cl
14	Rh	Cl

h to go to completion, it was possible to follow this transformation by ^1H NMR (in a sealed NMR tube) or by IR (in solution cells under an atmosphere of H_2). Most conveniently, the transformation of **11** in neat CH_2Cl_2 (or CD_2Cl_2) under H_2 was monitored; the species initially formed is the *mer*-amine–trihydride, $IrH_3[NH(SiMe_2CH_2PPh_2)_2]$,[26] **15**, which then apparently reacts with

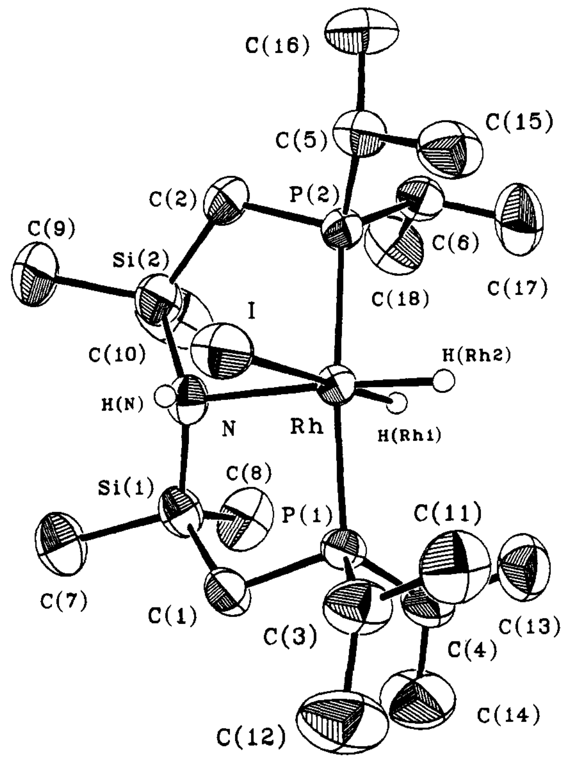

Figure 2. Molecular structure and numbering scheme for $RhH_2I[NH(SiMe_2CH_2P(i\text{-}Pr)_2)_2]$, **9b**.

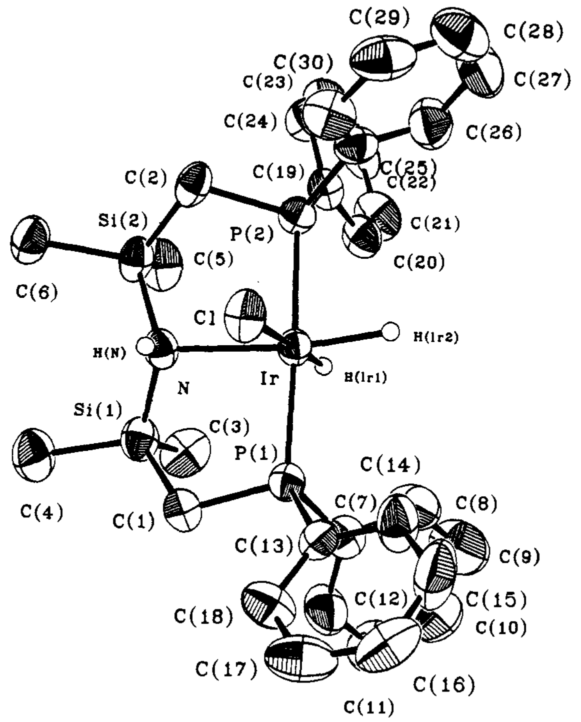

Figure 3. Molecular structure and numbering scheme for $IrH_2Cl[NH(SiMe_2CH_2PPh_2)_2]$, **13**.

CH_2Cl_2 to form $IrH_2Cl[NH(SiMe_2CH_2PPh_2)_2]$ and CH_3Cl. Presumably, the iodide and bromide derivatives as well as the

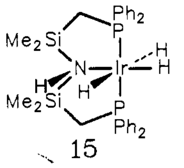

15

rhodium species **14** are formed in a similar fashion; however, formation of $IrH_2X[NH(SiMe_2CH_2PPh_2)_2]$ ($X = Br, I$) by this

---

(26) Fryzuk, M. D.; MacNeil, P. A. *Organometallics* **1983**, *2*, 682.

Table VIII. Summary of Intramolecular Hydrogen-Bonding from X-ray Crystallographic Data

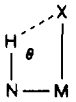

complex	H···X (Å)	van der Waal's separation[a] (Å)	θ (deg)
$IrH(CH_3)I[NH(SiMe_2CH_2P(i\text{-}Pr)_2)_2]$ (**5b**)	3.16 (9)	3.35	120 (9)
$RhH_2I[NH(SiMe_2CH_2P(i\text{-}Pr)_2)_2]$ (**9b**)	2.80 (4)	3.35	141 (4)
$IrH_2Cl[NH(SiMe_2CH_2PPh_2)_2]$ (**13**)	2.76 (6)	3.0	125 (6)

[a] Taken from ref 29.

route is somewhat complicated by further reactivity with CH_2Br_2 or CH_2I_2 to generate small amounts (~15%) of the amine-dihalide derivatives $Ir(H)X_2[NH(SiMe_2CH_2PPh_2)_2]$. As indicated by ^1H NMR, $^{31}P\{^1H\}$ NMR, and IR, these dihydrides are identical in every respect with the ultimate products of dihydrogen addition to the M(III) methyl halides. Of particular significance is that the stereochemistry of the iridium dihydrido chloride, $IrH_2Cl[NH(SiMe_2CH_2PPh_2)_2]$, **13**, prepared as in eq 6, is identical with that of $RhH_2I[NH(SiMe_2CH_2P(i\text{-}Pr)_2)_2]$ (**9b** in eq 5 and Figure 2), with cis hydrides and the amine N–H bond disposed syn to the metal halide group; the X-ray crystal structure of **13** is shown in Figure 3.

Yet another route to these types of complexes involves dihydrogen addition to the iridium(I) and rhodium(I) derivatives **16**[27] and **17**[28] (eq 7 and 8). Under mild conditions, the iridium and rhodium amine–dihydrides **13** and **14** are rapidly formed in virtually quantitative yields.

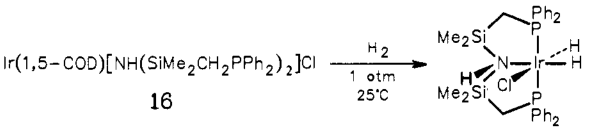

16 13 [7]

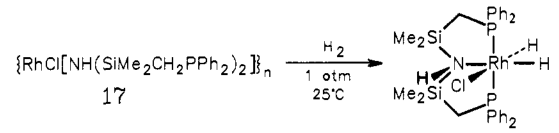

17 14 [8]

A startling feature of all of these transformations, which clearly must proceed by very different mechanisms, is that all of these amine–hydrides have the N–H and M–X moieties syn disposed. On the basis of the following spectroscopic and crystallographic data, we maintain that this is a consequence of intramolecular N-H···X hydrogen bonding.

Infrared Studies. In order to gauge the significance of any hydrogen-bonded interactions in these species, the N–H stretching frequencies of all of these derivatives were tabulated (Table II) and compared to the amine-trihydride **15**, $IrH_3[NH(SiMe_2CH_2PPh_2)_2]$. This latter species is a particularly useful standard in that it is an iridium(III) derivative, containing a coordinated N–H bond, for which no hydrogen bonding is possible. Consistent with these observations is the fact that ν_{N-H} for **15** (3258 cm^{-1}) is the highest value recorded for these complexes; in addition, it is the only N–H absorption which is sharp: all of the other N–H bands are very broad, as is characteristic of hydrogen-bonded systems.[3] For both the rhodium(III) and iridium(III) amine hydride, ν_{N-H} shifts to lower frequency as the halide becomes more strongly hydrogen bonded. This trend follows previously established patterns in both organic and organometallic species; a particularly appropriate comparison can be made to the cobalt(III) hexaamine, $[Co(NH_3)_6]X_3$, for which ν_{N-H} = 3070, 3120, and 3150 (X = Cl^-, Br^-, I^-, respectively).[6] The corresponding deuterides (Table II) show a shift of this stretching mode to lower frequency as expected. It is also noteworthy that the ratio ν_{N-H} ν_{N-D}, which ideally should be 1.369 for free molecules, is significantly lower in hydrogen-bonded systems.[2] Such is also the case for the amine hydrides; although the decrease in ν_{N-H}/ν_{N-D} (~1.32 → 1.34) is not large, it is quite comparable to weakly hydrogen-bonded organic molecules containing N–H functionalities.[2]

^1H NMR Chemical Shifts. The most noticeable feature of the downfield region of the ^1H NMR spectra of these complexes is the shift downfield of the N–H resonance as the strength of the hydrogen-bonded interaction increases (Table I). Specifically, δ_{N-H} (ppm, C_6D_6) for $IrH_2X[NH(SiMe_2CH_2PPh_2)_2]$ is ~2.4, 2.71, and 3.05 (X = I^-, Br^-, Cl^-, respectively), with the rhodium analogues following a similar trend (2.78, 3.07, and 3.38 ppm, respectively). Similar results have been noted in other hydrogen-bonded systems.[3,4,10]

X-ray Crystallographic Information. For the three amine-hydrides complexes **5b**, **9b**, and **13**, which were analyzed crystallographically, an interesting comparison can be made between the observed NH···X distances to those calculated from the sum of van der Waals radii[29] (Table VIII). In all cases, these distances are shorter than calculated nonbonded separations although in **5b** the difference is not statistically significant. An earlier study of a series of M(III) ethylenediamine complexes,[9] $[M(en)_3]X_3 \cdot nH_2O$ (M = Co^{3+}, Cr^{3+}, Rh^{3+}; X = Cl^-, Br^-, I^-), has shown that hydrogen bonding results in a similar contraction of N-H···X distances; the average values of these separations were found to be 2.63 (9) Å (X = Cl), 2.70 (10) Å (X = Br), and 2.97 (8) Å (X = I). Although these latter examples represent outer-sphere hydrogen-bonded systems, it is clear that the magnitude of this N-H···X contraction over calculated van der Waals distances is quite comparable to our intramolecularly hydrogen-bonded species.

Another point deserves comment. Typical hydrogen bonds have nearly linear N-H···X type arrays;[30] as is shown in Table VIII, the measured angles in our systems are considerably less being in the range 120–141°. The constraints of the octahedral geometry are undoubtedly the cause, but even so, this strained secondary interaction is still the controlling factor in the determination of stereochemistry and the stabilization of certain hydride complexes.

Conclusions

The following diverse transformations, discussed above in this work, all lead to octahedral amine–hydride derivatives of iridium(III) and rhodium(III): (i) dihydrogen activation by iridium(III) and rhodium(III) alkyl halides (eq 2-5), (ii) halide/hydride exchange of amine-trihydride complexes (eq 6), (iii) dihydrogen addition to preformed amine–halide derivatives (eq 7 and 8). In every case, isomerically pure, octahedral complexes

---

(27) The iridium complex $Ir(1,5\text{-}COD)[NH(SiMe_2CH_2PPh_2)_2]Cl$ has not been extensively structurally characterized but appears to be a fluxional, five-coordinate Ir(I) species analogous to those described in Shapley, J. R.; Osborn, J. A. *Acc. Chem. Res.* **1973**, *6*, 305.

(28) The rhodium(I) amine derivative $\{RhCl[NH(SiMe_2CH_2PPh_2)_2]\}_n$ is probably dimeric in solution; accurate solution molecular weight measurements (Signer) could not be obtained due to the low solubility of this species in typical organic solvents.

(29) Bondi, A. *J. Phys. Chem.* **1964**, *68*, 441.

(30) Cotton, F. A.; Wilkinson, G. *Advanced Inorganic Chemistry*, 4th ed., Wiley-Interscience: 1980; p 219.

are formed, all having remarkably similar stereochemistires. It is apparent therefore, that all of these reaction sequences are proceeding under thermodynamic control. The controlling factor is the formation of an intramolecular hydrogen bond between the N–H functionality and the coordinated halide moiety. Although the stereochemical control exerted by this type of hydrogen bonding is quite unusual, another result of this interaction is the stabilization of otherwise unstable metal hydrides. Thus the iridium(III) amine–trihydride complex **15** is stable in solution only when excess H_2 is present; loss of H_2 to generate the amide–dihydride $IrH_2[N(SiMe_2CH_2PPh_2)_2]$ occurs readily. However, upon substitution of one of the hydrides of **15** by a halide (eq 6), the resulting amine–dihydrides do not lose H_2 under vacuum even when heated to 80 °C. Even more remarkable is the corresponding rhodium chemistry. The rhodium(I) cyclooctene complex **12** is apparently unreactive to H_2 (1–4 atm) in aromatic or hydrocarbon solvents; after extended periods (several months), only decomposition to rhodium metal is observed. However, in chlorinated solvents, the reaction of H_2 with **12** generates the amine–dihydride complex **14**, which is stabilized by the presence of the intramolecular hydrogen bond.

All of these transformations involving H_2 are clearly quite complex; mechanistic investigations into these processes are currently in progress.

Acknowledgment. We thank NSERC and the Alfred P. Sloan Foundation for financial support. Johnson-Matthey is greatfully acknowledged for generous loans of $RhCl_3$ and $IrCl_3$. We also thank Professor James Trotter for the use of the diffractometer and structure solution programs.

Supplementary Material Available: Tables of calculated hydrogen coordinates and isotropic thermal parameters, final anisotropic thermal parameters, torsion angles, and intramolecular X···H interactions (14 pages); tables of observed and calculated structure factor amplitudes (102 pages). Ordering information is given on any current masthead page.

Quantitative Analyses of Biochemical Kinetic Resolution of Enantiomers. 2. Enzyme-Catalyzed Esterifications in Water–Organic Solvent Biphasic Systems

Ching-Shih Chen, Shih-Hsiung Wu, Gary Girdaukas, and Charles J. Sih*

Contribution from the School of Pharmacy, University of Wisconsin, Madison, Wisconsin 53706.
Received September 26, 1986

Abstract: New quantitative expressions, which relate the kinetic and thermodynamic parameters that govern the stereospecificity of enzyme-catalyzed resolution of enantiomers in biphasic aqueous–organic media, have been developed. The theoretical predictions have been verified experimentally, and the technical merit of this esterification methodology has been assessed in relation to the more conventional hydrolytic procedure.

Hydrolytic enzymes are valuable chiral catalysts for the resolution of racemic alcohols[1] and carboxylic acids[2] via enantiospecific hydrolyses of the corresponding esters. The reactions are usually conducted in aqueous media where the equilibrium position of the reaction is markedly shifted toward hydrolysis. Recently, the use of hydrolytic enzymes as catalysts for preparative ester synthesis has attracted considerable attention.[3] By replacing water with a biphasic aqueous–organic solvent reaction medium, the water activity is lowered and the thermodynamic equilibrium of the reaction is now shifted toward the synthetic direction.[4] Further, if the product(s) has good solubility in the organic phase and poor solubility in the aqueous phase while the reactants have the opposite solubility behavior, the reaction is shifted even further toward esterification. Several types of hydrolytic enzymes (proteases,[5] amidases,[6] lipases,[1,7] etc.) have now been shown to catalyze stereospecific condensation reactions in such aqueous–organic biphasic milieus. In particular, microbial lipases (EC 3.1.1.3) have been widely used for the resolution of racemic alcohols through enantiospecific esterifications.[1,7] These enzymes are relatively stable to nonpolar organic media and catalyze reactions efficiently at the lipid–water interface. However, the underlying physicochemical principles that govern enantiospecific esterification in biphasic systems have not yet been delineated.

In a previous paper,[8] we developed equations and useful graphs for the systematic treatment of kinetic resolution data of hydrolase-catalyzed irreversible reactions in water. As an extension of this work, we herein introduce new quantitative expressions to relate the kinetic and thermodynamic parameters that determine the stereospecificity of enzyme-catalyzed resolution of enantiomers in biphasic aqueous–organic media. Our theoretical predictions have been experimentally verified, and the technical merit of this esterification methodology can now be compared to the more conventional hydrolytic procedure.

Theory

In a normal hydrolytic reaction, water is also a substrate. Its high relative concentration (55.5 M) drives the reaction toward

---

(1) Langrand, G.; Baratti, J.; Buono, G.; Triantaphylides, C. *Tetrahedron Lett.* **1986**, *27*, 29.

(2) Gu, Q. M.; Chen, C. S.; Sih, C. J. *Tetrahedron Lett.* **1986**, *27*, 1763.

(3) (a) Kasche, V. *Enzyme Microb. Technol.* **1986**, *8*, 4. (b) Brink, L. E. S.; Tramper, J. *Biotech. Bioeng.* **1985**, *27*, 1258. (c) Halling, P. J. *Enzyme Microb. Technol.* **1984**, *6*, 513. (d) Carrea, G. *Trends Biotechnol.* **1984**, *2*, 102.

(4) Martinek, K.; Semenov, A. N.; Berezin, I. V. *Biochim. Biophys. Acta* **1981**, *658*, 76.

(5) (a) Fruton, J. S. *Adv. Enzymol. Rel. Areas Mol. Biol.* **1982**, *53*, 239. (b) Oyama, K.; Irino, S.; Harada, T.; Hagi, N. *Ann. N.Y. Acad. Sci.* **1984**, *434*, 95. (c) Markussen, J.; Vølund, A. In *Enzymes in Organic Synthesis*; Pitman: London, 1985; p 188.

(6) Kasche, V.; Haufler, U.; Riechmann, L. *Ann. N.Y. Acad. Sci.* **1984**, *434*, 99.

(7) (a) Langrand, G.; Secci, M.; Buono, G.; Baratti, J.; Triantaphylides, C. *Tetrahedron Lett.* **1985**, *26*, 1857. (b) Koshiro, S.; Sonomoto, K.; Tanaka, A.; Fukui, S. *J. Biotechnol.* **1985**, *2*, 47. (c) Kirchner, G.; Scollar, M. P.; Klibanov, A. M. *J. Am. Chem. Soc.* **1985**, *107*, 7072.

(8) Chen, C. S.; Fujimoto, Y.; Girdaukas, G.; Sih, C. J. *J. Am. Chem. Soc.* **1982**, *104*, 7294.

0002-7863/87/1509-2812$01.50/0